

OS-DiffVSR: Towards One-step Latent Diffusion Model for High-detailed Real-world Video Super-Resolution

Hanting Li*, Huacao Tang*, Jianhong Han, Tianxiong Zhou, Jilong Cui, Haizhen Xie, Yan Chen, Jie Hu[†]
Huawei Noah's Ark Lab

Abstract

Recently, latent diffusion models has demonstrated promising performance in real-world video super-resolution (VSR) task, which can reconstruct high-quality videos from distorted low-resolution input through multiple diffusion steps. Compared to image super-resolution (ISR), VSR methods needs to process each frame in a video, which poses challenges to its inference efficiency. However, video quality and inference efficiency have always been a trade-off for the diffusion-based VSR methods. In this work, we propose One-Step Diffusion model for real-world Video Super-Resolution, namely OS-DiffVSR. Specifically, we devise a novel adjacent frame adversarial training paradigm, which can significantly improve the quality of synthetic videos. Besides, we devise a multi-frame fusion mechanism to maintain inter-frame temporal consistency and reduce the flicker in video. Extensive experiments on several popular VSR benchmarks demonstrate that OS-DiffVSR can even achieve better quality than existing diffusion-based VSR methods that require dozens of sampling steps.

1. Introduction

With rapid iteration of video capture devices and improvement of Internet transmission speed, video content plays an increasingly important role in the digital media industry. The video super-resolution (VSR) task aims to convert low-resolution (LR) videos into high-resolution (HR) videos with rich details, thereby greatly improving video quality. real-world video degradations are very complex, including noise, blur, compression artifact, and other more complex compound degradations, which pose great challenges to VSR task.

Compared to image super-resolution (ISR), VSR methods needs to process each frame in a video sequence, which puts higher requirements on the model efficiency. VSR methods based on convolutional neural networks (CNNs)

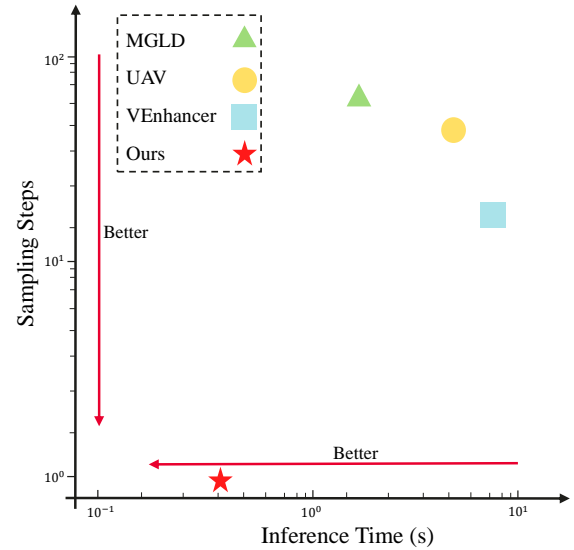


Figure 1. Comparison of model efficiency between existing diffusion-based VSR methods and our OS-DiffVSR.

[5, 38, 43] and recursive models [12, 13, 22] usually have higher reasoning efficiency, but are difficult to generate videos with rich details. Recently, diffusion models [1, 15, 33] have achieved remarkable success in various image and video synthesis tasks, such as text to video synthesis [8, 10], video editing [3, 4], and video restoration [21, 51, 59]. These methods can synthesize realistic videos through dozens or even hundreds of diffusion sampling steps, which makes the generation process time-consuming and difficult to meet the real-time requirements in many practical application scenarios.

Recently, compressing the sampling steps of vanilla diffusion models [15] based on stochastic differential equations (SDE) to fewer steps or even one step through distillation [54] or ordinary differential equation-based methods [25] has become the mainstream technical route to reduce the inference time. However, the performance of one-step diffusion-based methods still lag behind that of the multi-step methods.

Therefore, we propose **One-Step Diffusion** model for

*Equal contribution

[†]Corresponding author

real-world Video Super-Resolution (OS-DiffVSR) to extend the one-step ISR method (i.e., OSEDiff [46]) to VSR task. OS-DiffVSR greatly improves the quality of synthetic videos under one-step sampling setting, bringing the diffusion-based VSR method one step closer to practical applications. As shown in Figure 1, the proposed OS-DiffVSR has obvious advantages in both dimensions of inference time and sampling step when comparing with other multi-step diffusion-based VSR methods. Specifically, we devise a novel adjacent frame adversarial training (AFAT) paradigm, which trains the discriminator by conducting contrastive learning between adjacent frames. Under this training paradigm, OS-DiffVSR can even exceeding the performance of multi-step diffusion-based VSR methods. Besides, the proposed multi-frame fusion (MFF) module can improve the temporal consistency of the synthetic videos. In summary, our contributions are as follows:

- We proposed OS-DiffVSR, a one-step diffusion-based VSR method. OS-DiffVSR can produce compelling results comparable to multi-step diffusion models with one-step sampling.
- A novel adjacent frame adversarial training paradigm is proposed to improve the visual quality under one-step sampling setting.
- We devise a multi-frame fusion module to improve the temporal consistency of the synthetic videos.
- Extensive experiments on five popular VSR datasets demonstrate that OS-DiffVSR exceeds existing VSR methods. The effectiveness of our method is further corroborated by the qualitative comparisons.

2. Related Work

2.1. Video Super-Resolution

Traditional video super-resolution (VSR) methods have evolved from convolutional neural networks (CNNs) to transformers for handling temporal information. Early approaches predominantly relied on optical flow estimation [5, 18, 35, 49] or deformable convolutions [6, 16, 38, 42] for feature alignment and fusion. Later developments incorporated attention mechanisms [2, 22, 23] to facilitate information communication and integration within the network. However, these methods typically trained under simplified degradation models, resulting in limited generalization capabilities and a significant performance drop when confronted with complex real-world degradations. Subsequent research has focused on operating real-world VSR, as exemplified by DBVSR[29], RealBasicVSR[7], FastRealVSR[47], and RealViFormer[58].

Nevertheless, these approaches lack generative priors, which hinders their ability to synthesize sharp and realistic textures, ultimately constraining their overall performance. Recent progress in VSR has seen the rise of diffusion prior-

based methods, which have effectively addressed the limitations of traditional approaches in terms of detail sharpness and realism. However, a considerable disadvantage of almost all these methods is their dependence on iterative sampling procedures, leading to prohibitively high computational costs during inference. Our proposed method, conversely, harnesses the generative capabilities of diffusion models while necessitating only a single sampling step, achieving optimal inference efficiency without compromising generation quality.

2.2. Diffusion Prior for Video Super-Resolution

Employing diffusion-based generative priors in video super-resolution tasks allows for the synthesis of more authentic and refined details, ultimately contributing to an improved visual experience. A number of recent approaches have investigated the application of diffusion priors to video super-resolution. These approaches can be broadly categorized into two groups: those leveraging Text-to-Image (T2I) priors and those leveraging Text-to-Video (T2V) priors.

Many studies leverage pre-trained T2I models (e.g., Stable Diffusion[31] and its variants) as backbones and build upon them to adapt to the video super-resolution task. Common techniques employed include:

- Utilizing image super-resolution models as backbone: StableVSR [34], Upscale-A-Video [59], DiffVSR [20] and others are based on the SD \times 4 Upscaler[32].
- Incorporating motion information guidance [34, 59]: Extracting motion information via optical flow and integrating it into the diffusion sampling process to ensure temporal consistency.
- Constructing temporal modules[9, 20, 51]: Adding 3D convolutions, temporal attention mechanisms, etc., to pre-trained T2I models, such as U-Nets and VAE decoders, to explicitly model temporal correlations in videos.
- Adopting advanced architectures: SeedVR [41], based on SD3[11], employs shifted window based MM-DIT and causal video VAE, achieving effective super-resolution for arbitrary-length and resolution videos.
- Training-Free Methods: DiffIR2VR-zero [52] proposes a training-free method that achieves VSR through optical flow-guided hierarchical latent warping and hybrid flow-guided spatial-aware token merging.

In summary, VSR methods based on T2I priors capitalize on the powerful generative capabilities, supplemented by various optimization techniques tailored for video data, thereby achieving a good performance. A limitation of these approaches is their lack of optimization for inference efficiency, as they generally necessitate 30 to 50 sampling steps. The method proposed in this paper also falls into this category. But we utilize the research results on step distillation in the T2I community, achieving single-step video super-resolution, result in a substantial improvement in in-

ference efficiency.

Another approach is to directly leverage T2V models as priors. VEnhancer [14] and STAR [48] are both based on I2VGen-XL[57] and build upon it by adding 3D ControlNet[55]. VEnhancer[14] focuses primarily on enhancing the resolution of AIGC videos. STAR[48] utilizes local information enhancement modules and dynamic frequency loss to improve real-world video super-resolution performance. However, due to the immense parameter size of T2V models, methods based on T2V priors face challenges in terms of inference speed, with their inference latency typically higher than that of methods based on T2I models. Therefore, reducing the inference cost of T2V models is one of the future research directions in this field.

3. Method

Extending powerful and stable image synthesis diffusion model by adding trainable parameters has become a common paradigm for building VSR methods [51, 59]. Inspired by this idea, we built our method based on the latest ISR method (i.e., OSEDiff [46]). In this work we mainly focus on tackling two main challenges: 1) improving the *video quality* under one-step sampling conditions, 2) improving the *temporal consistency* of synthesized videos.

To address the above two challenges, we proposed OS-DiffVSR. As shown in Figure 2, OS-DiffVSR mainly consists of three key components, which are multi-frame fusion module, Denoising UNet, and the adjacent frame adversarial training paradigm. For a given low-resolution video sequence consisting of N frames $\mathcal{V}_{LR} = \{I_1^L, I_2^L, \dots, I_N^L\}$, Our goal is to reconstruct the corresponding high-resolution video $\hat{\mathcal{V}}_{HR} = \{\hat{I}_1^H, \hat{I}_2^H, \dots, \hat{I}_N^H\}$ from \mathcal{V}_{LR} . Firstly, we use the VAE encoder to map each frame into the latent space. For each latent feature Z_i^L , We fuse the information of warped adjacent frames (i.e., Z_{i-1}^w and Z_{i+1}^w) through the proposed MFF module. Since the frame fusion is completed before being fed to UNet, the redundant computational overhead of intermediate-layer fusion is avoided, which allows OS-DiffVSR to fuse temporal information with minimal computational overhead. Then the fused latent embed Z_i^f is fed into the denoising UNet together with the text prompt and the fixed time step T , which is consistent with the noise prediction process in OSEDiff. The denoised latent feature \hat{Z}_i^H is decoded by the frozen VAE decoder to obtain the high-resolution output \hat{I}_i^H . In addition to the mean square error (MSE) loss and perceptual loss commonly used in super-resolution tasks, we also propose a novel adjacent frame adversarial training paradigm to guide the generator to synthesize more realistic details through the previous frame.

During the training process, the VAE encoder and UNet are fine-tuned with low-rank adaptation (LoRA), while the multi-frame fusion module and the discriminator (i.e., DI-

NOv2 [28]) are trained under full-parameter tuning setting. Only the VAE decoder is frozen throughout the training process.

3.1. Preliminary: Latent Diffusion Model

Diffusion models [15] are a class of generative models that convert Gaussian noise into specific data samples through an iterative inverse Markov process. While the latent diffusion models (LDMs) [33] first map the data into the low-dimensional latent space, and then completes the diffusion and denoising process in the latent space. This paradigm has greatly promoted the development of high-dimensional data (e.g., images and video) generation [1, 30].

During the training stage, given a latent feature $Z^L \sim p_{LR}$ of a low-resolution image. The noised latent feature Z_t^L at the t -th diffusion step can be calculated by,

$$Z_t^L = \alpha_t Z^L + \beta_t \epsilon, \quad (1)$$

where α_t and β_t , $t \in \{1, 2, \dots, T\}$ define a noise schedule. Follow the one-step sampling process in [46], the denoised latent feature \hat{Z}^H can be obtained by a UNet ϵ_θ that can predict the noise in Z_t^L , which can be formulated as,

$$\hat{Z}^H = \frac{Z^L - \beta_T \epsilon_\theta(Z^L; T, c)}{\alpha_T}. \quad (2)$$

Where c denotes text descriptions corresponding to each frame, and T represents the total number of diffusion steps.

3.2. Adjacent Frame Adversarial Training Paradigm

Adversarial training is a common strategy to improve performance of super-resolution models [44]. By training a discriminator to distinguish from the ground truth and generated HR results, the discriminator can help the SR model synthesize more high-detailed images [43]. Although vanilla adversarial training paradigm has achieved promising result in the super-resolution tasks, in the VSR task, it can still be improved in the following aspects: 1) vanilla adversarial training paradigm do not fully exploit the information from other frames especially adjacent frame; 2) Traditional discriminator can only implicitly optimize the generator by narrowing the gap between real data and synthetic data distribution, but cannot provide direct guidance for specific samples. Therefore, we propose a novel adjacent frame adversarial training paradigm to train our OS-DiffVSR. We choose DINOv2 [28], a foundation model widely used in computer vision tasks, as our discriminator.

Discriminator: The optimization goal of our discriminator is to distinguish the super-resolution result of the current frame \hat{I}_i^H from ground truth I_i^H based on the previous frame. By conducting contrastive learning between real

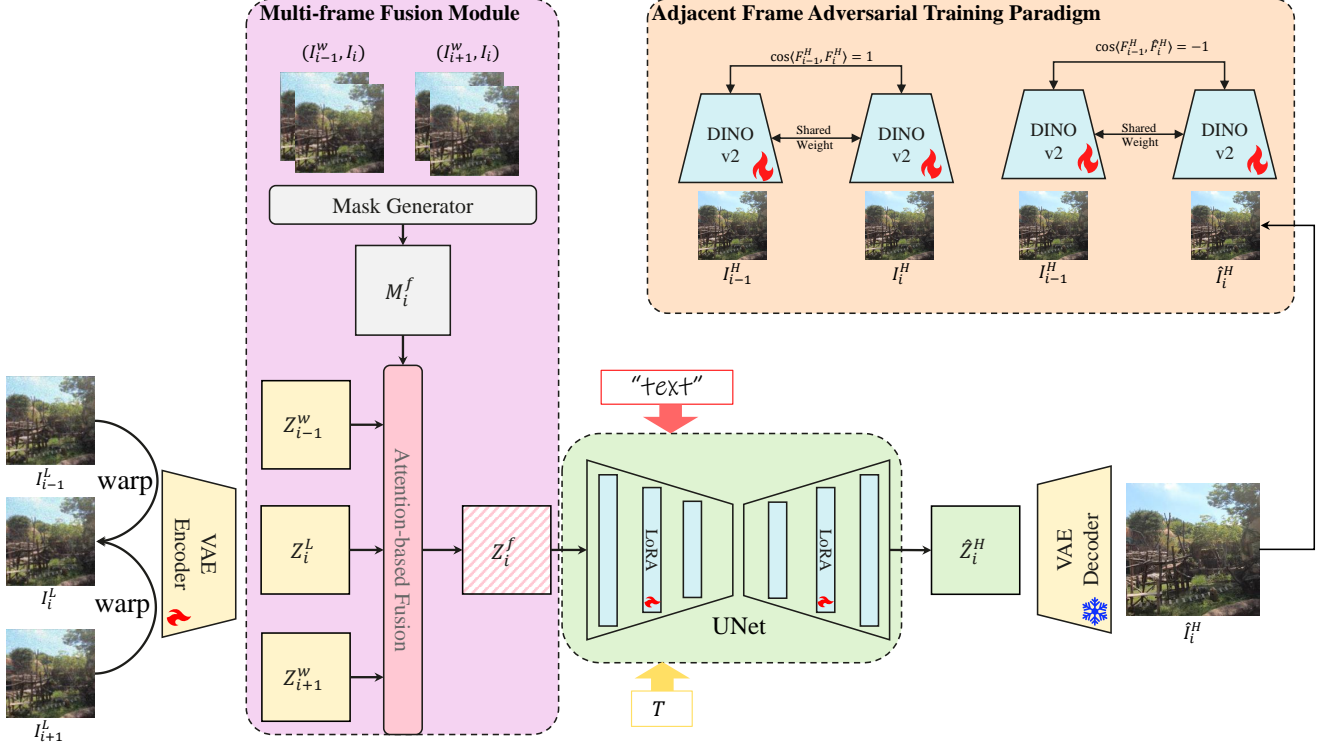


Figure 2. Overview of the proposed OS-DiffVSR. The overall framework mainly contains a generator composed of multi-frame fusion module and UNet and a adjacent frame discriminator based on DINOv2 [28].

adjacent frame pairs (i.e., I_{i-1}^H and I_i^H) and fake adjacent frame pairs (i.e., I_{i-1}^H and \hat{I}_i^H), the discriminator use the previous frame as a reference to distinguish the synthesized video, thus guiding the generator to generate a more realistic video. Specially, by utilizing the every output token of DINOv2, we can perform adversarial training at patch level, and the loss function of the discriminator can be defined as,

$$\mathcal{L}_D = -\frac{1}{PQ} \sum_{p=1}^P \sum_{q=1}^Q \log \frac{e^{\langle F_{i-1,p,q}^H, F_{i,p,q}^H \rangle / \tau}}{e^{\langle F_{i-1,p,q}^H, F_{i,p,q}^H \rangle / \tau} + e^{\langle F_{i-1,p,q}^H, \hat{F}_{i,p,q}^H \rangle / \tau}}, \quad (3)$$

with

$$\begin{aligned} F_i^H &= \mathcal{F}_\theta(I_i^H), \\ \hat{F}_i^H &= \mathcal{F}_\theta(\hat{I}_i^H). \end{aligned} \quad (4)$$

Where $\langle \cdot, \cdot \rangle$ stands for the cosine similarity between two vectors and τ denotes the temperature parameter used to control the margin between real and fake frame pairs. I_i^H and \hat{I}_i^H represent the i -th frame of the ground truth video and the synthetic video, respectively. \mathcal{F}_θ is our discriminator DINOv2 and $F_{i,p,q}^H$ is the patch-level feature at saptial position (p, q) extracted by the discriminator.

Generator: The training objective of the generator is to maximize the similarity between the synthetic frame and

the real adjacent frame. Therefore, the loss function of the generator can be written as,

$$\mathcal{L}_G = -\frac{1}{PQ} \sum_{p=1}^P \sum_{q=1}^Q \langle F_{i-1,p,q}^H, \hat{F}_{i,p,q}^H \rangle. \quad (5)$$

Focal Mean Square Error Since our discriminator can perform patch-level scoring based on the cosine similarity between I_i^H and \hat{I}_i^H , we further use these scores to locate spatial locations with poor visual quality, thereby enhancing the reconstruction constraints of these spatial regions. Inspired by the focal loss [24] that can make the network pay more attention to the classes with less samples, we propose focal mean square loss to make the model focus on optimizing areas where the visual quality is poor. Based on the above insights, the focal mean square (FMSE) loss can be defined as,

$$\mathcal{L}_{fmse} = S_i^\gamma \left\| I_i^H - \hat{I}_i^H \right\|_2, \quad (6)$$

with

$$S_i = \frac{1 - \langle F_{i-1}^H, \hat{F}_i^H \rangle}{2} \uparrow_{\times n}. \quad (7)$$

Where $S_i \in [0, 1]$ denotes the pixel-wise modulating factor of the i -th frame and $\gamma \geq 0$ represent the focusing parameter.

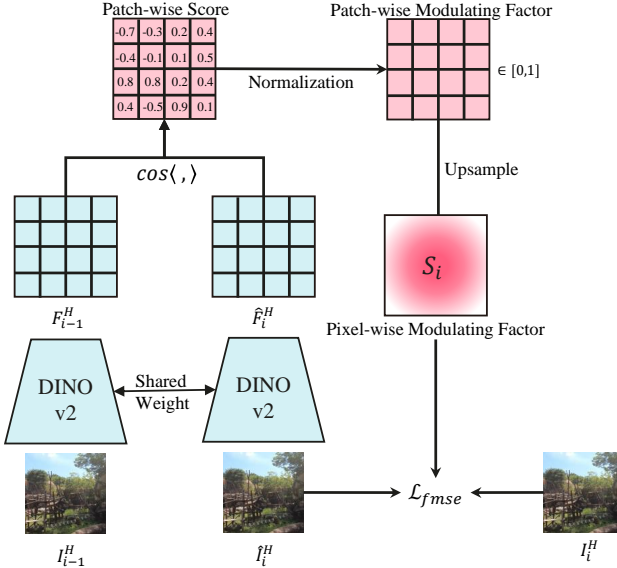


Figure 3. Illustration of the proposed focal mean square error.

$\uparrow_{\times n}$ is n times upsampling, which is used to upscale the patch-level feature to the same size as the original image resolution ($n=14$ in our work).

3.3. Multi-frame Fusion Module

The most significant difference between ISR and VSR is that VSR methods can obtain the temporal information from adjacent frames (e.g., previous frame and successor frame). Making full use of these information can not only improve the temporal consistency, but also improve the visual quality. In order to better fuse multi-frame information, we first utilize optical flow to align adjacent frames to the current frame:

$$\begin{aligned} I_{i-1}^w &= \text{Warp}(I_{i-1}^L, OF_{b,i-1}^L), \\ I_{i+1}^w &= \text{Warp}(I_{i+1}^L, OF_{f,i+1}^L). \end{aligned} \quad (8)$$

Where $OF_{b,i}^L$ and $OF_{f,i}^L$ are the backward and forward optical flow of the i -th frame computed on the low-resolution sequence, respectively. Then the VAE encoder E_{vae} is used to map the warped frame together with the current frame into the latent space:

$$\begin{aligned} Z_{i-1}^w &= E_{vae}(I_{i-1}^w), \\ Z_{i+1}^w &= E_{vae}(I_{i+1}^w), \\ Z_i^L &= E_{vae}(I_i^L). \end{aligned} \quad (9)$$

Then we conduct attention-based fusion on these three latent features, the attention weight of the m -th head can be calculated by,

$$A_m = \text{Softmax}\left(\frac{Q_m K_m^T}{\sqrt{d_k}}\right), \quad (10)$$

where

$$\begin{aligned} Q_m &= W_m^Q[Z_{i-1}^w, Z_i^L, Z_{i+1}^w], \\ K_m &= W_m^K[Z_{i-1}^w, Z_i^L, Z_{i+1}^w]. \end{aligned} \quad (11)$$

d_k denotes the dimension of the key vector K_m . Then the fused latent feature can be calculated by,

$$Z_i^f = \frac{\tilde{Z}_{i-1}^w + \tilde{Z}_i^L + \tilde{Z}_{i+1}^w}{3} M_i^f \downarrow_{\times n} + (1 - M_i^f \downarrow_{\times n}) Z_i^L, \quad (12)$$

where $\downarrow_{\times n}$ denotes n times downsampling,

$$[\tilde{Z}_{i-1}^w, \tilde{Z}_i^L, \tilde{Z}_{i+1}^w] = \frac{\sum_{m=1}^{N_h} A_m}{N_h} [Z_{i-1}^w, Z_i^L, Z_{i+1}^w], \quad (13)$$

and

$$M_i^f = \begin{cases} 1 & \text{if } e^{-\alpha(\|I_{i-1}^w - I_i^L\|_1 + \|I_{i+1}^w - I_i^L\|_1)} > \mu, \\ 0 & \text{if } e^{-\alpha(\|I_{i-1}^w - I_i^L\|_1 + \|I_{i+1}^w - I_i^L\|_1)} \leq \mu. \end{cases} \quad (14)$$

N_h is the number of attention heads and μ is the fusion threshold. M_i^f denotes a hard mask calculated from the warping error between adjacent frames that can restrict the MFF module to do frame fusion only in aligned regions and $\alpha > 0$ is a scaling factor. It is worth noting that we do not map the input latent feature into representation subspace, as did in vanilla multi-head self-attention [39]. Such a design allows the fused latent features to still be in the original VAE latent space, thus making better use of pre-training weights.

3.4. Loss Function

In order to improve the temporal consistency of the synthetic video, we additionally introduce warp loss defined in [19]:

$$\mathcal{L}_{warp} = M_i \left\| \hat{I}_i^H - \text{Warp}(I_{i-1}^H, OF_{b,i-1}^H) \right\|_2, \quad (15)$$

where

$$M_i = e^{-\alpha(\|I_i^H - \text{Warp}(I_{i-1}^H, OF_{b,i-1}^H)\|_1)}. \quad (16)$$

The function of M_i is the same as M_i^f , e.g., the loss is only calculated in the region where the warp alignment is accurate.

Given the above defined generator loss \mathcal{L}_G , focal mean square error loss \mathcal{L}_{fmse} , the commonly used perceptual loss \mathcal{L}_{lpips} and the warp loss \mathcal{L}_{warp} , the total loss for training OS-DiffVSR is defined as,

$$\mathcal{L}_{total} = \omega_1 \mathcal{L}_G + \omega_2 \mathcal{L}_{fmse} + \omega_3 \mathcal{L}_{lpips} + \omega_4 \mathcal{L}_{warp}, \quad (17)$$

where $\omega_1, \omega_2, \omega_3$, and ω_4 are empirically set to 1, 1, 2, and 2, respectively.

Datasets	Metrics	Real-ESRGAN[43]	SD $\times 4$ Upscaler[32]	RealBasicVSR[7]	MGLD[51]	VEnhancer[14]	UAV[59]	Ours
REDS4	PSNR \uparrow	22.225	21.511	23.479	22.780	18.907	21.889	21.789
	CLIP-IQA \uparrow	0.465	0.193	0.379	0.411	0.218	0.251	0.544
	MUSIQ \uparrow	66.601	27.901	65.259	66.476	41.9984	52.372	67.286
	MANIQA \uparrow	0.609	0.357	0.623	0.645	0.4799	0.487	0.646
	DOVER \uparrow	0.617	0.264	0.631	0.697	0.603	0.481	0.627
UDM10	PSNR \uparrow	26.428	24.535	27.756	26.594	20.027	25.768	25.308
	CLIP-IQA \uparrow	0.502	0.240	0.469	0.500	0.376	0.378	0.619
	MUSIQ \uparrow	62.429	32.325	62.835	62.923	55.653	54.275	66.071
	MANIQA \uparrow	0.552	0.350	0.564	0.569	0.497	0.460	0.579
	DOVER \uparrow	0.776	0.330	0.784	0.769	0.714	0.667	0.785
SPMCS	PSNR \uparrow	22.059	21.337	22.961	22.357	17.196	21.366	21.347
	CLIP-IQA \uparrow	0.492	0.238	0.442	0.469	0.343	0.419	0.585
	MUSIQ \uparrow	66.910	33.183	67.576	67.401	51.986	61.052	66.322
	MANIQA \uparrow	0.574	0.381	0.574	0.610	0.533	0.510	0.623
	DOVER \uparrow	0.675	0.303	0.604	0.628	0.449	0.600	0.664
YouHQ40	PSNR \uparrow	23.485	21.448	23.910	23.332	18.824	23.035	22.719
	CLIP-IQA \uparrow	0.468	0.289	0.482	0.543	0.380	0.434	0.598
	MUSIQ \uparrow	59.719	28.392	64.336	65.626	49.137	54.751	65.142
	MANIQA \uparrow	0.507	0.328	0.546	0.579	0.442	0.472	0.583
	DOVER \uparrow	0.860	0.509	0.836	0.858	0.754	0.767	0.829
VideoLQ	NIQE \downarrow	4.081	8.560	3.702	3.652	5.460	5.426	3.455
	CLIP-IQA \uparrow	0.377	0.267	0.381	0.366	0.288	0.212	0.575
	MUSIQ \uparrow	56.240	23.748	59.805	56.528	43.751	38.711	65.071
	MANIQA \uparrow	0.507	0.321	0.548	0.536	0.415	0.379	0.585
	DOVER \uparrow	0.744	0.345	0.749	0.747	0.655	0.556	0.755

Table 1. Quantitative comparison with state-of-the-art methods on synthetic datasets (REDS4, SPMCS, UDM10, YouHQ40) and realworld datasets (VideoLQ). The best and second-best results are marked in red and blue, respectively.

4. Experiments

4.1. Datasets and Implementaiton Details

Datasets. We use REDS dataset [27] as our training set, which contains 266 videos with resolution 1280×720 . Following OSEDiff [46], we employ the degradation process in RealESRGAN [43] to generate low-quality images for $4\times$ super-resolution setting. For evaluation, we test on four synthetic datasets (i.e., REDS4 [27], UDM10 [36], SPMCS [53] and YouHQ40 [59]) and a real-world dataset (i.e., VideoLQ [7]). According to other mainstream video super-resolution works, during the inference, we generate LR for systhetic datasets with the degradation from RealBasicVSR [7].

Training Details. We implement our method using PyTorch and train the model with a batch size of 8 for 150 epochs. During the training, HR images are randomly cropped into 512×512 patches and then utilized to generate corresponding LR images. To train the generator part, we use AdamW [26] optimizer with initial learning rate of 1e-5 and weight decay of 1e-8. The LoRA rank is set to 32 by default. RAFT [37] is used to generate the optical flow to warp the previous and successor LR frames. We use SGD optimizer to synchronously train the DINOv2-S [28] discriminator. The SGD optimizer will warm up 500 iterations to reach the learning rate of 5e-4. The temperature

coefficient τ and the fusion threshold μ is set to 100 and 0.4, respectively.

Evaluation Metrics. Frame quality is measured by both fidelity-based metric (PSNR) and perceptual-driven metrics (CLIP-IQA [40], MUSIQ [17], MANIQA [50], NIQE [56]). Overall video quality is measured by DOVER [45] and the temporal consistency is evaluated by the warping error(E_{warp}^*) [19].

4.2. Comparison with State-of-the-Arts

We compare OS-DiffVSR with several state-of-the art VSR methods, including Real-ESRGAN [43], SD $\times 4$ Upscaler [32], RealBasicVSR [7], MGLD [51], VEnhancer [14], and Upscale-a-video (UAV) [59].

Quantitative Evaluation. We evaluate our method on five datasets, including four synthetic degradation datasets and one real-world dataset. As shown in Table 1, CNN-based methods, such as RealBasicVSR and RealESRGAN, tend to over-smooth when dealing with high-frequency degradation (e.g., noise), so they usually achieve a higher PSNR than diffusion-based methods [20]. Besides, PSNR are primarily designed to measure pixel-level fidelity, while our method focuses on perceptual quality. For the perception-driven metrics, OS-DiffVSR achieves the best performance on almost all datasets with much less infer-

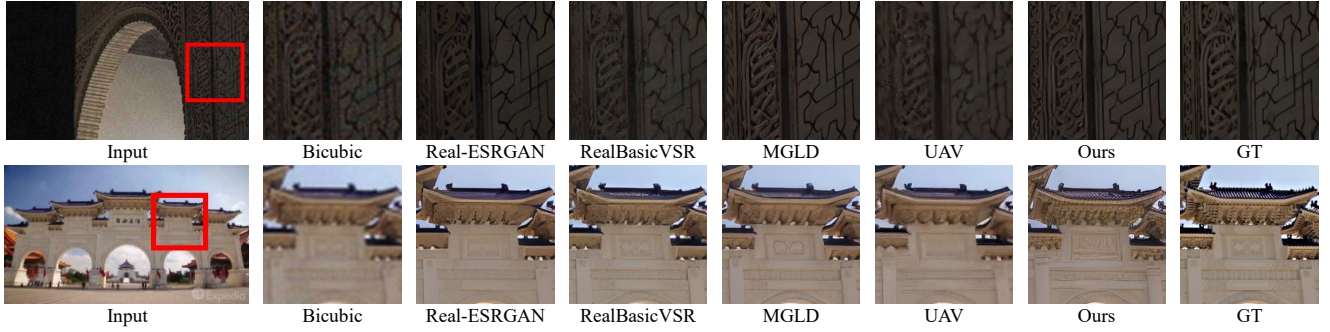


Figure 4. Qualitative comparisons on synthetic LR videos from UDM10 and SPMCS datasets. OS-DiffVSR can recover more realistic and clear architectural details (zoom-in for better view).

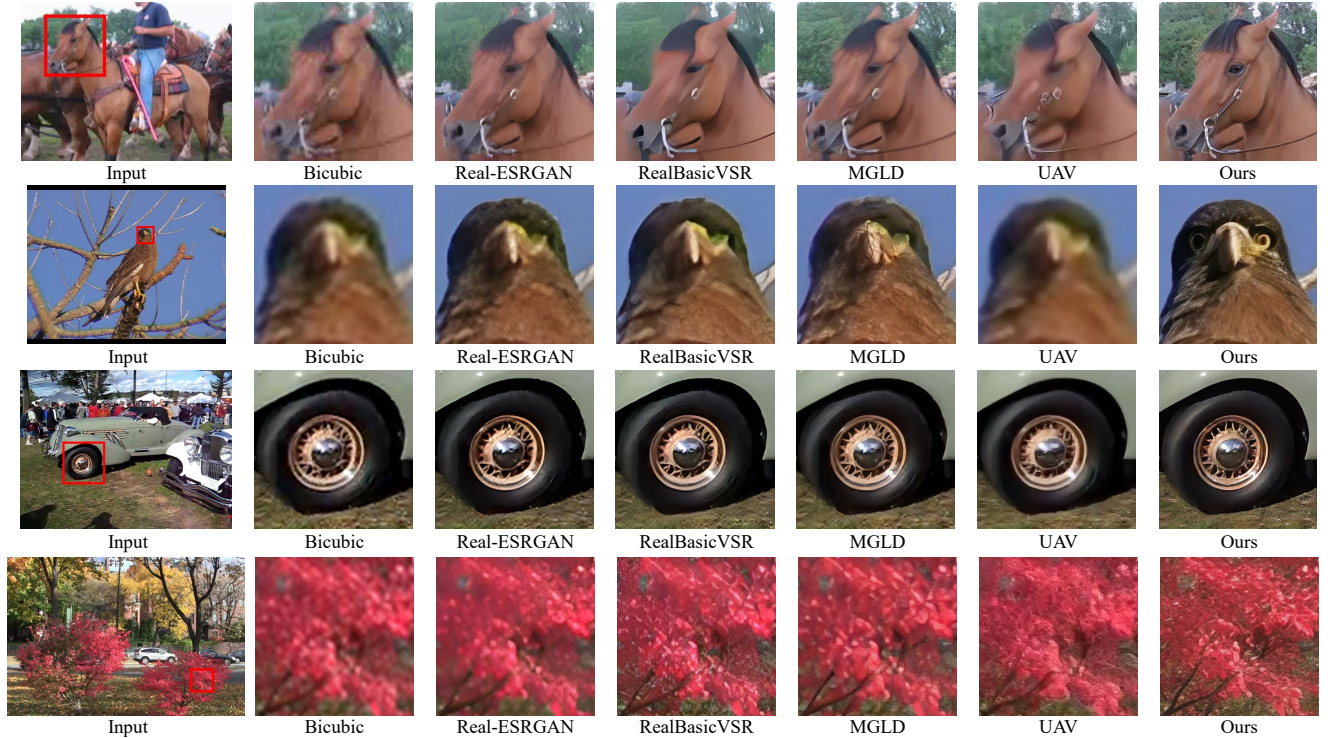


Figure 5. Qualitative comparisons on real-world LR videos from VideoLQ dataset. OS-DiffVSR can synthesize animals, plants and objects with rich details (zoom-in for better view).

ence time than existing multi-step diffusion-based methods (e.g., MGLD, UAV, and VEnhancer). It is worth noting that our method achieves best performance on all metrics on the real-world dataset VideoLQ, which prove that OS-DiffVSR can cope well with various degradations in real-world videos. Besides, We also achieve competitive results on the DOVER, which is the latest video quality metric.

Qualitative Evaluation. We present visualization results on synthetic datasets (i.e., UDM10 and SPMCS) in Figure 4 and a real-world dataset in Figure 5 to further demonstrate the effectiveness of OS-DiffVSR. The results shows that our method can effectively remove various types of degradation and restore clear and realistic details. As shown in Figure 4,

OS-DiffVSR can generate more realistic and reasonable architectural details. The results on real-world datasets show that the good generalization ability of OS-DiffVSR enables it to effectively deal with various complex degradations in the real world. More visual comparisons can be found in the supplementary materials.

4.3. Ablation Study

We conduct ablation experiments on UDM10 dataset [36] to validate the effectiveness of different components of OS-DiffVSR, including the adjacent frame adversarial training paradigm and multi-frame fusion module. More detailed ablation experiments can refer to supplementary materials.

Settings	PSNR↑	CLIP-IQA↑	MUSIQ↑	MANIQA↑
Baseline	26.414	0.530	62.158	0.566
Vanilla GAN	24.597	0.598	67.834	<u>0.592</u>
AFAT (class token)	<u>25.971</u>	0.576	63.771	0.578
AFAT (patch token)	25.590	0.612	66.115	0.591
AFAT (patch token) + FMSE	25.503	<u>0.606</u>	<u>66.529</u>	0.594

Table 2. Evaluation of the adjacent frame adversarial training paradigm. The videos synthesized under the **vanilla GAN** training paradigm have serious pseudo-textures (see supplementary materials for examples).

Settings	NIQE↓	DOVER↑	$E_{warp}^* \downarrow$
OSEDiff	4.049	0.780	1.917
Baseline	<u>3.766</u>	0.761	2.003
MFF	3.868	<u>0.784</u>	<u>1.843</u>
MFF+Warp Loss	3.727	0.785	1.805

Table 3. Evaluation of the multi-frame adversarial training paradigm.

μ	CLIP-IQA↑	MUSIQ↑	DOVER↑	$E_{warp}^* \downarrow$
1.0	0.607	64.981	0.745	1.862
0.8	0.599	65.206	0.766	1.830
0.6	0.629	<u>66.135</u>	0.772	1.744
0.4	0.619	66.072	0.785	1.805
0.2	<u>0.626</u>	66.264	0.785	1.801
0.0	0.618	66.123	<u>0.781</u>	<u>1.792</u>

Table 4. Evaluation of different fusion threshold μ . $\mu=1.0$ means the MFF module is not introduced.

Evaluation of Adjacent Frame Adversarial Training. We evaluate the effectiveness of the proposed AFAT and the focal MSE loss in Table 2. The baseline setting stands for only utilizing the vanilla MSE loss and the perceptual loss for fine-tuning OSEDiff on our training set. The results show that the perceptual-driven metrics can be greatly improved when the AFAT is introduced. In particular, although the vanilla adversarial training paradigm (i.e., Vanilla GAN) achieves comparable results in perceptual-driven metrics to AFAT, its PSNR significantly dropped by 1.817dB compared to the baseline, which is reflected in the serious pseudo-textures in the synthetic Videos (some relevant examples can be found in the supplementary material). Besides, we also found that utilizing the patch token of DINOv2 to conduct patch-level adversarial training can achieve better performance than using the class token, and the FMSE loss can further boosting the final performance.

Evaluation of Multi-Frame Fusion Module. We evaluate the effectiveness of MFF module in Table 3. The baseline setting denotes fine-tuning OSEDiff under AFAT

paradigm (i.e., the last row of Table 2). The results show that the proposed MFF module can significantly improve the overall video quality and temporal consistency at the cost of a subtle drop of single frame quality. Besides, introducing the warp loss can further reduce the warp error that measures the temporal consistency.

Studies on the Fusion Threshold. We conducted comprehensive studies on the effectiveness of the fusion threshold μ in Table 4. It is worth noting that $\mu=0$ is equivalent to not using the MFF module, so it can serve as a baseline for comparison. The results show that as the fusion threshold decreases (i.e., the fusion area expands), the overall video quality and temporal consistency of the method show an overall upward trend. However, a too small μ will lead to the fusion of more misaligned information. For example, the visual quality degrades when $\mu=0$. Therefore, we choose $\mu=0.4$ as our default setting.

Some works have observed that despite the wide use of WE for temporal consistency evaluation, it may not be able to faithfully reflect the real human perception on a video. For example, WE could be easily attacked by blurring the sequence, resulting much better WE scores but lower video quality [51]. In Table 4, we can observe that there is a trade-off between visual quality and temporal consistency. The more details the synthetic video has, the worse the temporal consistency of the video is.

5. Conclusion

We propose OS-DiffVSR, a one-step diffusion-based video super-resolution method in this work. For improving the perceptual quality, we devise a novel adjacent frame adversarial training paradigm, which can provide more direct guidance for generator by introducing previous frame as a reference. Besides, we introduce a multi-frame fusion module to utilize the information from adjacent frame, thus improving the temporal consistency and the overall video quality. Extensive experiments demonstrate that OS-DiffVSR can achieve state-of-the-art performance with much lower inference time than existing diffusion-based methods. The visualization results show that OS-DiffVSR can generate high-detail and realistic videos.

References

[1] Andreas Blattmann, Robin Rombach, Huan Ling, Tim Dockhorn, Seung Wook Kim, Sanja Fidler, and Karsten Kreis. Align your latents: High-resolution video synthesis with latent diffusion models. In *Proceedings of the IEEE/CVF Conference on Computer Vision and Pattern Recognition*, pages 22563–22575, 2023. 1, 3

[2] Jiezhang Cao, Yawei Li, Kai Zhang, and Luc Van Gool. Video super-resolution transformer. *arXiv preprint arXiv:2106.06847*, 2021. 2

[3] Duygu Ceylan, Chun-Hao P Huang, and Niloy J Mitra. Pix2video: Video editing using image diffusion. In *Proceedings of the IEEE/CVF International Conference on Computer Vision*, pages 23206–23217, 2023. 1

[4] Wenhao Chai, Xun Guo, Gaoang Wang, and Yan Lu. Stable-Video: Text-driven consistency-aware diffusion video editing. In *Proceedings of the IEEE/CVF International Conference on Computer Vision*, pages 23040–23050, 2023. 1

[5] Kelvin CK Chan, Xintao Wang, Ke Yu, Chao Dong, and Chen Change Loy. BasicVSR: The search for essential components in video super-resolution and beyond. In *Proceedings of the IEEE/CVF Conference on Computer Vision and Pattern Recognition*, pages 4947–4956, 2021. 1, 2

[6] Kelvin CK Chan, Xintao Wang, Ke Yu, Chao Dong, and Chen Change Loy. Understanding deformable alignment in video super-resolution. In *Proceedings of the AAAI Conference on Artificial Intelligence*, pages 973–981, 2021. 2

[7] Kelvin CK Chan, Shangchen Zhou, Xiangyu Xu, and Chen Change Loy. Investigating tradeoffs in real-world video super-resolution. In *Proceedings of the IEEE/CVF Conference on Computer Vision and Pattern Recognition*, pages 5962–5971, 2022. 2, 6

[8] Tsai-Shien Chen, Chieh Hubert Lin, Hung-Yu Tseng, Tsung-Yi Lin, and Ming-Hsuan Yang. Motion-conditioned diffusion model for controllable video synthesis. *arXiv preprint arXiv:2304.14404*, 2023. 1

[9] Zhikai Chen, Fuchen Long, Zhaofan Qiu, Ting Yao, Wengang Zhou, Jiebo Luo, and Tao Mei. Learning spatial adaptation and temporal coherence in diffusion models for video super-resolution. In *Proceedings of the IEEE/CVF Conference on Computer Vision and Pattern Recognition*, pages 9232–9241, 2024. 2

[10] Patrick Esser, Johnathan Chiu, Parmida Atighehchian, Jonathan Granskog, and Anastasis Germanidis. Structure and content-guided video synthesis with diffusion models. In *Proceedings of the IEEE/CVF International Conference on Computer Vision*, pages 7346–7356, 2023. 1

[11] Patrick Esser, Sumith Kulal, Andreas Blattmann, Rahim Entezari, Jonas Müller, Harry Saini, Yam Levi, Dominik Lorenz, Axel Sauer, Frederic Boesel, et al. Scaling rectified flow transformers for high-resolution image synthesis. In *Proceedings of the International Conference on Machine Learning*, 2024. 2

[12] Dario Fuoli, Shuhang Gu, and Radu Timofte. Efficient video super-resolution through recurrent latent space propagation. In *Proceedings of the IEEE/CVF International Conference on Computer Vision*, pages 3476–3485. IEEE, 2019. 1

[13] Muhammad Haris, Gregory Shakhnarovich, and Norimichi Ukita. Recurrent back-projection network for video super-resolution. In *Proceedings of the IEEE/CVF Conference on Computer Vision and Pattern Recognition*, pages 3897–3906, 2019. 1

[14] Jingwen He, Tianfan Xue, Dongyang Liu, Xinqi Lin, Peng Gao, Dahua Lin, Yu Qiao, Wanli Ouyang, and Ziwei Liu. Venhancer: Generative space-time enhancement for video generation. *arXiv preprint arXiv:2407.07667*, 2024. 3, 6

[15] Jonathan Ho, Ajay Jain, and Pieter Abbeel. Denoising diffusion probabilistic models. In *Proceedings of the Advances in Neural Information Processing Systems*, pages 6840–6851, 2020. 1, 3

[16] Younghyun Jo, Seoung Wug Oh, Jaeyeon Kang, and Seon Joo Kim. Deep video super-resolution network using dynamic upsampling filters without explicit motion compensation. In *Proceedings of the IEEE/CVF Conference on Computer Vision and Pattern Recognition*, pages 3224–3232, 2018. 2

[17] Junjie Ke, Qifei Wang, Yilin Wang, Peyman Milanfar, and Feng Yang. MUSIQ: Multi-scale image quality transformer. In *Proceedings of the IEEE/CVF International Conference on Computer Vision*, pages 5148–5157, 2021. 6

[18] Tae Hyun Kim, Mehdi SM Sajjadi, Michael Hirsch, and Bernhard Scholkopf. Spatio-temporal transformer network for video restoration. In *Proceedings of the European Conference on Computer Vision*, pages 106–122, 2018. 2

[19] Wei-Sheng Lai, Jia-Bin Huang, Oliver Wang, Eli Shechtman, Ersin Yumer, and Ming-Hsuan Yang. Learning blind video temporal consistency. In *Proceedings of the European Conference on Computer Vision*, pages 170–185, 2018. 5, 6

[20] Xiaohui Li, Yihao Liu, Shuo Cao, Ziyan Chen, Shaobin Zhuang, Xiangyu Chen, Yinan He, Yi Wang, and Yu Qiao. DiffVSR: Enhancing real-world video super-resolution with diffusion models for advanced visual quality and temporal consistency. *arXiv preprint arXiv:2501.10110*, 2025. 2, 6

[21] Yizhou Li, Zihua Liu, Yusuke Monno, and Masatoshi Okutomi. TDM: Temporally-Consistent Diffusion Model for All-in-One Real-World Video Restoration. In *International Conference on Multimedia Modeling*, pages 155–169. Springer, 2025. 1

[22] Jingyun Liang, Yuchen Fan, Xiaoyu Xiang, Rakesh Ranjan, Eddy Ilg, Simon Green, Jiezhang Cao, Kai Zhang, Radu Timofte, and Luc Van Gool. Recurrent video restoration transformer with guided deformable attention. In *Proceedings of the Advances in Neural Information Processing Systems*, pages 378–393, 2022. 1, 2

[23] Jingyun Liang, Jiezhang Cao, Yuchen Fan, Kai Zhang, Rakesh Ranjan, Yawei Li, Radu Timofte, and Luc Van Gool. VRT: A video restoration transformer. *IEEE Transactions on Image Processing*, 2024. 2

[24] Tsung-Yi Lin, Priya Goyal, Ross Girshick, Kaiming He, and Piotr Dollár. Focal loss for dense object detection. In *Proceedings of the IEEE/CVF International Conference on Computer Vision*, pages 2980–2988, 2017. 4

[25] Xingchao Liu, Chengyue Gong, and Qiang Liu. Flow straight and fast: Learning to generate and transfer data with rectified flow. *arXiv preprint arXiv:2209.03003*, 2022. 1

[26] Ilya Loshchilov and Frank Hutter. Decoupled weight decay regularization. *arXiv preprint arXiv:1711.05101*, 2017. 6

[27] Seungjun Nah, Sungyong Baik, Seokil Hong, Gyeongsik Moon, Sanghyun Son, Radu Timofte, and Kyoung Mu Lee. Ntire 2019 challenge on video deblurring and super-resolution: Dataset and study. In *Proceedings of the IEEE/CVF Conference on Computer Vision and Pattern Recognition workshops*, pages 0–0, 2019. 6

[28] Maxime Oquab, Timothée Darcret, Théo Moutakanni, Huy Vo, Marc Szafraniec, Vasil Khalidov, Pierre Fernandez, Daniel Haziza, Francisco Massa, Alaaeldin El-Nouby, et al. DINOv2: Learning robust visual features without supervision. *arXiv preprint arXiv:2304.07193*, 2023. 3, 4, 6

[29] Jinshan Pan, Haoran Bai, Jiangxin Dong, Jiawei Zhang, and Jinhui Tang. Deep blind video super-resolution. In *Proceedings of the IEEE/CVF International Conference on Computer Vision*, pages 4811–4820, 2021. 2

[30] Dustin Podell, Zion English, Kyle Lacey, Andreas Blattmann, Tim Dockhorn, Jonas Müller, Joe Penna, and Robin Rombach. SDXL: Improving latent diffusion models for high-resolution image synthesis. *arXiv preprint arXiv:2307.01952*, 2023. 3

[31] Robin Rombach, Andreas Blattmann, Dominik Lorenz, Patrick Esser, and Björn Ommer. High-resolution image synthesis with latent diffusion models, 2021. 2

[32] Robin Rombach, Andreas Blattmann, Dominik Lorenz, Patrick Esser, and Björn Ommer. High-resolution image synthesis with latent diffusion models. In *Proceedings of the IEEE/CVF Conference on Computer Vision and Pattern Recognition (CVPR)*, pages 10684–10695, 2022. 2, 6

[33] Robin Rombach, Andreas Blattmann, Dominik Lorenz, Patrick Esser, and Björn Ommer. High-resolution image synthesis with latent diffusion models. In *Proceedings of the IEEE/CVF Conference on Computer Vision and Pattern Recognition*, pages 10684–10695, 2022. 1, 3

[34] Claudio Rota, Marco Buzzelli, and Joost van de Weijer. Enhancing perceptual quality in video super-resolution through temporally-consistent detail synthesis using diffusion models. In *Proceedings of the European Conference on Computer Vision*, pages 36–53. Springer, 2024. 2

[35] Mehdi SM Sajjadi, Raviteja Vemulapalli, and Matthew Brown. Frame-recurrent video super-resolution. In *Proceedings of the IEEE/CVF Conference on Computer Vision and Pattern Recognition*, pages 6626–6634, 2018. 2

[36] Xin Tao, Hongyun Gao, Renjie Liao, Jue Wang, and Jiaya Jia. Detail-revealing deep video super-resolution. In *Proceedings of the IEEE/CVF International Conference on Computer Vision*, pages 4472–4480, 2017. 6, 7

[37] Zachary Teed and Jia Deng. RAFT: Recurrent all-pairs field transforms for optical flow. In *Computer Vision–ECCV 2020: 16th European Conference, Glasgow, UK, August 23–28, 2020, Proceedings, Part II 16*, pages 402–419. Springer, 2020. 6

[38] Yapeng Tian, Yulun Zhang, Yun Fu, and Chenliang Xu. TDAN: Temporally-deformable alignment network for video super-resolution. In *Proceedings of the IEEE/CVF Conference on Computer Vision and Pattern Recognition*, pages 3360–3369, 2020. 1, 2

[39] Ashish Vaswani, Noam Shazeer, Niki Parmar, Jakob Uszkoreit, Llion Jones, Aidan N Gomez, Łukasz Kaiser, and Illia Polosukhin. Attention is all you need. In *Proceedings of the Advances in Neural Information Processing Systems*, 2017. 5

[40] Jianyi Wang, Kelvin CK Chan, and Chen Change Loy. Exploring clip for assessing the look and feel of images. In *Proceedings of the AAAI Conference on Artificial Intelligence*, pages 2555–2563, 2023. 6

[41] Jianyi Wang, Zhijie Lin, Meng Wei, Yang Zhao, Ceyuan Yang, Chen Change Loy, and Lu Jiang. SeedVR: Seeding infinity in diffusion transformer towards generic video restoration. *arXiv preprint arXiv:2501.01320*, 2025. 2

[42] Xintao Wang, Kelvin CK Chan, Ke Yu, Chao Dong, and Chen Change Loy. EDVR: Video restoration with enhanced deformable convolutional networks. In *Proceedings of the IEEE/CVF Conference on Computer Vision and Pattern Recognition workshops*, pages 0–0, 2019. 2

[43] Xintao Wang, Liangbin Xie, Chao Dong, and Ying Shan. RealESRGAN: Training real-world blind super-resolution with pure synthetic data. In *Proceedings of the IEEE/CVF International Conference on Computer Vision*, pages 1905–1914, 2021. 1, 3, 6

[44] Zhihao Wang, Jian Chen, and Steven CH Hoi. Deep learning for image super-resolution: A survey. *IEEE Transactions on Pattern Analysis and Machine Intelligence*, 43(10):3365–3387, 2020. 3

[45] Haoning Wu, Erli Zhang, Liang Liao, Chaofeng Chen, Jingwen Hou, Annan Wang, Wenxiu Sun, Qiong Yan, and Weisi Lin. Exploring video quality assessment on user generated contents from aesthetic and technical perspectives. In *Proceedings of the IEEE/CVF International Conference on Computer Vision*, pages 20144–20154, 2023. 6

[46] Rongyuan Wu, Lingchen Sun, Zhiyuan Ma, and Lei Zhang. One-step effective diffusion network for real-world image super-resolution. In *Proceedings of the Advances in Neural Information Processing Systems*, pages 92529–92553, 2025. 2, 3, 6

[47] Liangbin Xie, Xintao Wang, Shuwei Shi, Jinjin Gu, Chao Dong, and Ying Shan. Mitigating artifacts in real-world video super-resolution models. In *Proceedings of the AAAI Conference on Artificial Intelligence*, pages 2956–2964, 2023. 2

[48] Rui Xie, Yinhong Liu, Penghao Zhou, Chen Zhao, Jun Zhou, Kai Zhang, Zhenyu Zhang, Jian Yang, Zhenheng Yang, and Ying Tai. Star: Spatial-temporal augmentation with text-to-video models for real-world video super-resolution. *arXiv preprint arXiv:2501.02976*, 2025. 3

[49] Tianfan Xue, Baian Chen, Jiajun Wu, Donglai Wei, and William T Freeman. Video enhancement with task-oriented flow. *International Journal of Computer Vision*, 127:1106–1125, 2019. 2

[50] Sidi Yang, Tianhe Wu, Shuwei Shi, Shanshan Lao, Yuan Gong, Mingdeng Cao, Jiahao Wang, and Yujiu Yang.

MANIQA: Multi-dimension attention network for no-reference image quality assessment. In *Proceedings of the IEEE/CVF Conference on Computer Vision and Pattern Recognition*, pages 1191–1200, 2022. 6

[51] Xi Yang, Chenhang He, Jianqi Ma, and Lei Zhang. Motion-guided latent diffusion for temporally consistent real-world video super-resolution. In *Proceedings of the European Conference on Computer Vision*, pages 224–242. Springer, 2024. 1, 2, 3, 6, 8

[52] Chang-Han Yeh, Chin-Yang Lin, Zhixiang Wang, Chi-Wei Hsiao, Ting-Hsuan Chen, Hau-Shiang Shiu, and Yu-Lun Liu. DiffIR2VR-Zero: Zero-shot video restoration with diffusion-based image restoration models. *arXiv preprint arXiv:2407.01519*, 2024. 2

[53] Peng Yi, Zhongyuan Wang, Kui Jiang, Junjun Jiang, and Jiayi Ma. Progressive fusion video super-resolution network via exploiting non-local spatio-temporal correlations. In *Proceedings of the IEEE/CVF International Conference on Computer Vision*, pages 3106–3115, 2019. 6

[54] Tianwei Yin, Michaël Gharbi, Richard Zhang, Eli Shechtman, Fredo Durand, William T Freeman, and Taesung Park. One-step diffusion with distribution matching distillation. In *Proceedings of the IEEE/CVF Conference on Computer Vision and Pattern Recognition*, pages 6613–6623, 2024. 1

[55] Lvmin Zhang, Anyi Rao, and Maneesh Agrawala. Adding conditional control to text-to-image diffusion models. 3

[56] Lin Zhang, Lei Zhang, and Alan C Bovik. A feature-enriched completely blind image quality evaluator. *IEEE Transactions on Image Processing*, 24(8):2579–2591, 2015. 6

[57] Shiwei Zhang, Jiayu Wang, Yingya Zhang, Kang Zhao, Hangjie Yuan, Zhiwu Qin, Xiang Wang, Deli Zhao, and Jingren Zhou. I2Vgen-XL: High-quality image-to-video synthesis via cascaded diffusion models. *arXiv preprint arXiv:2311.04145*, 2023. 3

[58] Yuehan Zhang and Angela Yao. RealVifomer: Investigating attention for real-world video super-resolution. In *Proceedings of the European Conference on Computer Vision*, pages 412–428. Springer, 2024. 2

[59] Shangchen Zhou, Peiqing Yang, Jianyi Wang, Yihang Luo, and Chen Change Loy. Upscale-a-video: Temporal-consistent diffusion model for real-world video super-resolution. In *Proceedings of the IEEE/CVF Conference on Computer Vision and Pattern Recognition*, pages 2535–2545, 2024. 1, 2, 3, 6